Nonlinear Analysis: Modelling and Control, 2009, Vol. 14, No. 1, 73–84

Free Convection MHD Flow with Thermal Radiation from an Impulsively-Started Vertical Plate

G. Palani[1], **I. A. Abbas**[2]

[1]Department of Mechanical Engineering, Inha University
Incheon - 402-751, Republic of Korea
gpalani32@yahoo.co.in

[2]Department of Mathematics, Faculty of Science, Sohag University
82524, Sohag, Egypt
ibrahim.abbas@sci.sohag.edu.eg; ibrabbas7@yahoo.com

Received: 2008-06-18 **Revised:** 2008-10-06 **Published online:** 2009-03-10

Abstract. This paper investigates the combined effects of magnetohydrodynamics and radiation on free convection flow past an impulsively started isothermal vertical plate with Rosseland diffusion approximation. The fluid considered is a gray, absorbing-emitting radiation but a non-scattering medium, with approximate transformations the boundary layer governing the flow are reduced to non-dimensional equations valid in the free convection regime. The dimensionless governing equations are solved by the finite element method.

Keywords: magnetohydrodynamics, radiation, finite element, skin friction, vertical plate.

Nomenclature

B_o^2	magnetic field induction	T	dimensionless temperature
C_p	specific heat constant pressure	T'_∞	temperature of fluid away from the plate
g	acceleration due to gravity		
Gr	thermal Grashof number	T'_w	temperature of the plate
k	thermal conductivity of the fluid	t'	time
k^*	mean absorption coefficient	t	dimensionless time
M	magnetic field parameter	u_0	velocity of the plate
N	Rosseland or Stark conduction radiation parameter	u, v	velocity components in x, y-directions respectively
Nu_x	dimensionless local Nusselt number	U, V	dimensionless velocity components in X, Y-directions respectively
$\overline{Nu}$	dimensionless average Nusselt number	x	spatial coordinate along the plate
Pr	Prandtl number	X	dimensionless spatial coordinate along the plate
T'	temperature		

y	spatial coordinate normal to the plate	Y	dimensionless spatial coordinate normal to the plate

Greek symbols

α	thermal diffusivity	μ	coefficient of viscosity
β	volumetric coefficient of thermal expansion	ν	kinematic viscosity
		σ	electrical conductivity
τ_X	local skin friction	σ^*	Stefan Boltzmann constant
$\overline{\tau}$	average skin friction	ρ	density

Subscripts

w	conditions on the wall	∞	free stream conditions

1 Introduction

The experimental and theoretical studies of magnetohydrodynamics flows are important from a technological point of view, because they have many applications, as for examples in magnetohydrodynamics electrical power generation, geophysics etc.

The influence of a magnetic field on viscous incompressible flow of electrically conducting fluid is of importance in many applications such as extrusion of plastics in the manufacture of Rayon and Nylon, purification of crude oil, magnetic materials processing, glass manufacturing control processes and the paper industry in different geophysical cases etc., In many process industries, the cooling of threads or sheets of some polymer materials is of importance in the production line. Magneto convection plays an important role in various industrial applications including magnetic control of molten iron flow in the steel industry and liquid metal cooling in nuclear reactors.

Free convection heat transfer due to the simultaneous action of buoyancy and induced magnetic forces was investigated by Sparrow and Cess [1]. They observed that the free convection heat transfer to liquid metals may be significantly affected by the presence of a magnetic field.The interaction of thermal radiation with free convection heat transfer was studied by Cess [2]. The effects of a transversely applied magnetic field on the flow of an electrically conducting fluid past an impulsively started vertical plate for the case when the plate is isothermal studied by Soundalgekar et al. [3], when it was characterized by variable surface temperature [4]. The dimensionless governing equations were solved by the Laplace transform technique. The flow of viscous incompressible electrically conducting fluid past an impulsively started infinite vertical isothermal plate was studied by Soundalgekar and Abdulla Ali [5] by employing the finite difference technique. Kumari and Nath [6] studied the development of the asymmetric flow of a viscous electrically conducting fluid in the forward stagnation point region of a two-dimensional body and over a stretching surface with an applied magnetic field, when the external stream or the stretching surface was set into an impulsive motion from the rest. Vajravelu [7] considered the exact solution for the hydrodynamic boundary layer flow and heat transfer over a continuous, moving and vertical flat surface with uniform suction, internal heat generation

and absorption.

Radiative flows are encountered in countless industrial and environmental processes e.g., heating and cooling chambers, fossil fuel combustion and energy processes, evaporation from large open water reservoirs, astrophysical flows and solar power technology. Soundalgekar and Takhar [8] considered the radiative free convective flow of an optically thin gray-gas past a semi-infinite vertical plate. Radiation effects on mixed convection along an isothermal vertical plate were studied by Hossain and Takhar [9]. Raptis and Perdikis [10] studied the effects of thermal radiation and free convection flow past a moving vertical plate. Muthucumaraswamy and Ganesan [11] studied radiation effects on flow past an impulsively started infinite vertical plate with variable temperatures using the Laplace transform technique.

On the other hand,the Magnetohydrodynamics flow past a plate by the presence of radiation was studied by Raptis and Massalas [12]. An analytical solution for the mean temperature, velocity and the magnetic field have been arrived and the effects of radiation on temperature are discussed. The combined effects of thermal radiation flux, thermal conductivity, Reynolds number and non-Darcian (Forcheimmer drag and Brinkman boundary resistance) body forces on a steady laminar boundary layer flow along a vertical surface in an idealized geological porous medium were investigated by Takhar et al. [13].The effects of thermal radiation and porous drag forces on the natural convection heat and mass transfer of a viscous, incompressible, gray, absorbing emitting fluid flowing past an impulsively started moving vertical plate adjacent to a non-Darcian porous regime was studied by Anwar et al. [14].

However, the free convection MHD flow with thermal radiation from an impulsively started semi-infinite isothermal vertical plate has not received the attention of any researcher.The object of the present investigation is to study the combined effects of MHD and Radiation on the free convection flow past a semi-infinite vertical plate,when the fluid is compressible, viscous and electrically conducting.The fluid considered is a gray,radiation, absorbing, emitting but non-scattering medium and the Rosseland approximation is used to describe the radiative heat transfer in the energy equation. The set of non-dimensional governing equations are solved by the finite element method.

2 Mathematical analysis

We considered the unsteady flow of a viscous incompressible and electrical conducting fluid past an impulsively started semi-infinite vertical plate. The x-axis is taken along the plate in the vertical direction and the y-axis is taken normal to the plate. Initially, the plate and the fluid were at the same temperature in a stationary condition. At time $t' > 0$ the plate is given an impulse motion in the vertical direction against the gravitational force with constant velocity u_0 and its temperature was instanteously raised to T'_w which was thereafter maintained constant. It is assumed that the plate is electrically non conducting and the magnetic field is applied uniform and perpendicular to the plate. The magnetic Reynolds number on the flow is taken to be small so that the induced magnetic field is negligible. The effects of viscous dissipation are neglected in the energy equation. All the

fluid properties are assumed to be constant except the influence of the density variation with temperature is considered only in the body force term.

Under the above assumption, the flow is governed by the following set of equations.

$$\frac{\partial u}{\partial x}+\frac{\partial v}{\partial y}=0, \tag{1}$$

$$\frac{\partial u}{\partial t'}+u\frac{\partial u}{\partial x}+v\frac{\partial u}{\partial y}=g\beta\big(T'-T'_\infty\big)+\nu\,\frac{\partial^2 u}{\partial y^2}-\frac{\sigma B_o^2}{\rho}u, \tag{2}$$

$$\rho C_p\left[\frac{\partial T'}{\partial t'}+u\frac{\partial T'}{\partial x}+v\frac{\partial T'}{\partial y}\right]=k\frac{\partial^2 T'}{\partial y^2}-\frac{\partial q_r}{\partial y}, \tag{3}$$

where the Rosseland approximation (Brewster [15]) is used, which leads to

$$q_r=\frac{-4\sigma^*}{3k^*}\frac{\partial T'^4}{\partial y}. \tag{4}$$

The initial and boundary conditions are

$$\begin{array}{lllll} t'\le 0\colon & u=0, & v=0, & T'=T'_\infty, & \\ t'>0\colon & u=u_0, & v=0, & T'=T'_w & \text{at } y=0,\\ & u=0 & T'=T'_\infty & \text{at } x=0, & \\ & u\to 0, & T\to T_\infty, & \text{as } y\to\infty. & \end{array} \tag{5}$$

We assumed that the temperature differences within the flow are sufficiently small such that T'^4 may be expressed as a linear function of the temperature. This was accomplished by expanding T'^4 in a Taylor series about T'_∞ and neglecting higher-order terms. Thus

$$T'^4\cong 4T'^3_\infty T'-3T'^4_\infty. \tag{6}$$

Using (4) and (6) in (3) gives

$$\rho C_p\left[\frac{\partial T'}{\partial t'}+u\frac{\partial T'}{\partial x}+v\frac{\partial T'}{\partial y}\right]=k\frac{\partial^2 T'}{\partial y^2}+\frac{16\sigma^* T'^3_\infty}{3k^*}\frac{\partial^2 T'}{\partial y^2}. \tag{7}$$

On introducing the following non-dimensional quantities:

$$\begin{array}{l} X=\dfrac{xu_0}{\nu},\quad Y=\dfrac{yu_0}{\nu},\quad U=\dfrac{u}{u_0},\quad V=\dfrac{v}{u_0},\\ t=\dfrac{t'u_0^2}{\nu}\quad T=\dfrac{T'-T'_\infty}{T'_w-T'_\infty},\quad Gr=\dfrac{g\beta\nu(T'_w-T'_\infty)}{u_0^3},\\ Pr=\dfrac{\mu C_p}{k},\quad N=\dfrac{k^*k}{4\sigma^* T'^3_\infty},\quad M=\dfrac{\sigma B_o^2\nu}{\rho u_o^2} \end{array} \tag{8}$$

equations (1), (2) and (7) are reduced to the following dimensionless form

$$\frac{\partial U}{\partial X} + \frac{\partial V}{\partial Y} = 0, \tag{9}$$

$$\frac{\partial U}{\partial t} + U\frac{\partial U}{\partial X} + V\frac{\partial U}{\partial Y} = Gr\, T + \frac{\partial^2 U}{\partial Y^2} - MU, \tag{10}$$

$$\frac{\partial T}{\partial t} + U\frac{\partial T}{\partial X} + V\frac{\partial T}{\partial Y} = \frac{1}{Pr}\frac{(3N+4)}{(3N)}\frac{\partial^2 T}{\partial Y^2}. \tag{11}$$

The corresponding initial and boundary conditions in a dimensionless form are as follows:

$$\begin{array}{lllll} t \le 0: & U = 0, & V = 0, & T = 0, & \text{for all } y, \\ t > 0: & U = 1, & V = 0, & T = 1, & \text{at } Y = 0, \\ & U = 0, & T = 0 & \text{at } X = 0, & \\ & U \to 0, & T \to 0 & \text{as } Y \to \infty. & \end{array} \tag{12}$$

3 Finite element method

The governing equations (9)–(11) are unsteady, coupled and non-linear with initial and boundary conditions (12). They are solved numerically by finite element method (FEM). In the method of finite element, the region of integration of the governing equations is divided into rectangular meshes formed by two sets of lines, parallel to the coordinate axis. Here the region of integration is considered as a rectangle with sides $x_{max}(= 1.0)$ and $y_{max}(= 7.0)$ where y_{max} corresponds to $(y = \infty)$ which lies very well outside the momentum and thermal boundary layers. The numerical values of the dependent variables like velocity U, V and the temperature T are obtained at the interesting points which are called degrees of freedom. The weak formulations of the non-dimensional governing equations are derived. The set of independent test functions to consist of the velocity U, V and the temperature T is prescribed. The governing equations are multiplied by independent weighting functions and then are integrated over the spatial domain within the boundary. Applying integration by parts and making use of the divergence theorem reduce the order of the spatial derivatives and allows for the application of the boundary conditions. The same shape functions were defined piecewise on the elements. Using the Galerkin procedure, the unknown fields U, V and T and the corresponding weighting functions were approximated by the same shape functions. The last step towards the finite element discretization is to choose the element type and the associated shape functions. Eight nodes of quadrilateral elements were used. The unknown fields were approximated either by linear shape functions, which were defined by four corner nodes or by quadratic shape functions, which were defined by all of the eight nodes (two-dimensional quadrilateral elements). On other hand the unknown fields were approximated either by linear shape functions, which were defined by three corner nodes or by quadratic shape functions, which were defined by all of the six nodes (two-dimensional triangular elements). The shape function is usually denoted by the letter N and is usually the

coefficient that appears in the interpolation polynomial. A shape function was written for each individual node of a finite element and has the property that its magnitude is 1 at that node and 0 for all other nodes in that element. We assumed that the master element has its local coordinates in the range $[-1, 1]$. In our case, the two-dimensional quadrilateral elements were used, which given by

linear shape functions:

$$N_1 = \frac{1}{4}(1-\xi)(1-\eta), \quad N_2 = \frac{1}{4}(1+\xi)(1-\eta),$$
$$N_3 = \frac{1}{4}(1+\xi)(1+\eta), \quad N_4 = \frac{1}{4}(1-\xi)(1+\eta),$$

quadratic shape functions:

$$N_1 = \frac{1}{4}(1-\xi)(1-\eta)(-1-\xi-\eta), \quad N_5 = \frac{1}{2}\left(1-\xi^2\right)(1-\eta),$$
$$N_2 = \frac{1}{4}(1+\xi)(1-\eta)(-1+\xi-\eta), \quad N_6 = \frac{1}{2}(1+\xi)\left(1-\eta^2\right),$$
$$N_3 = \frac{1}{4}(1+\xi)(1+\eta)(-1+\xi+\eta), \quad N_7 = \frac{1}{2}\left(1-\xi^2\right)(1+\eta),$$
$$N_4 = \frac{1}{4}(1-\xi)(1+\eta)(-1-\xi+\eta), \quad N_8 = \frac{1}{2}(1-\xi)\left(1-\eta^2\right).$$

4 Results and discussion

In order to ascertain the accuracy of our numerical results, the present study was compared with the available exact solution in the literature. The velocity profiles for $Gr = 0.2$, $M = 2, 4$, $N = 0$ and $t = 0.5, 1.0$ compared with the available exact solution of Soundalgekar [3], is shown in Fig. 1. It was observed that the agreement with the theoretical solution of velocity is excellent.

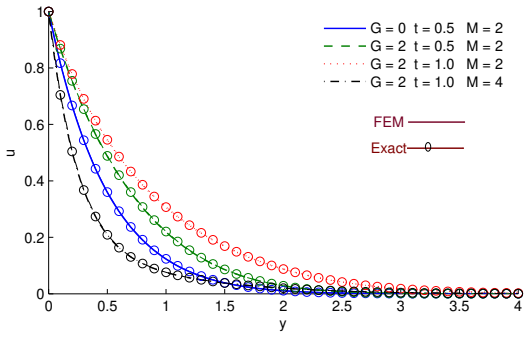

Fig. 1. Comparison of velocity profiles.

The velocity profiles for different values of the Grashof number, Prandtl number, magnetic field parameter and radiation parameter are shown in Fig. 2. The velocity profiles decreased with an increasing Prandtl number. Physically, this is true because the increase in the Prandtl number is due to increase in the viscosity of the fluid which makes the fluid thick and hence causes a decrease in the velocity of the fluid.It was observed that an increase in Gr, leads to a rise in the values of velocity due to enhancement in buoyancy force. As M increases, the Lorentz force, which opposes the flow, also increases and leads to enchanted deceleration of the flow. This result qualitatively agrees with the expectations, since the magnetic field exerts a retarding force on the free convection flow. It was observed that an increase in the radiation parameter lead to a fall in the velocity.

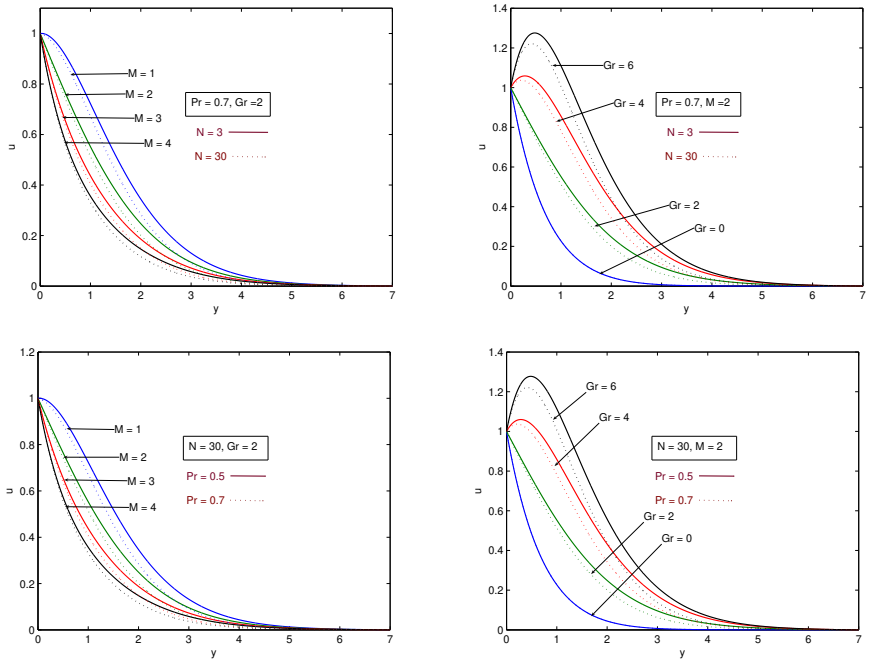

Fig. 2. Transient velocity profiles at $X = 1.0$.

The temperature profiles were calculated numerically from equation 11 for different values of parameters occurring into the problem are shown in Fig. 3. The effect of the Prandtl number is very important in the temperature field. A fall in temperature occurs due to an increasing value of the Prandtl number. This is in agreement with the physical fact that the thermal boundary layer thickness decreases with increasing Pr. The effects of a magnetic field parameter on the temperature profile was nil. It is seen that the temperature decreases as the radiation parameter N increases. This result qualitatively agrees with expectations, since the effect of radiation is to decrease the rate of energy transport to the fluid, thereby decreasing the temperature of the fluid.

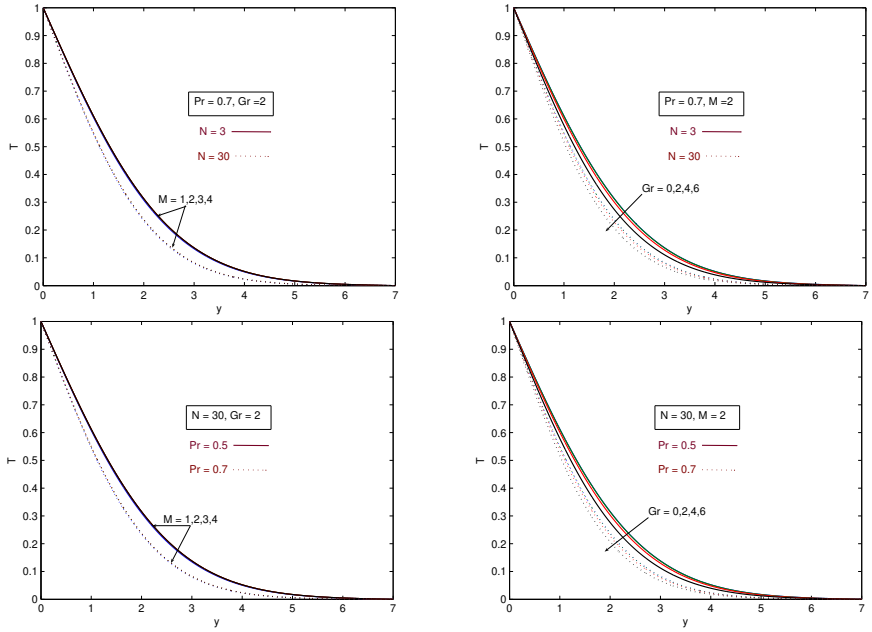

Fig. 3. Transient temperature profiles at $X = 1.0$.

Knowing the velocity and the temperature field, it is customary to study the skin-friction and the rate of heat transfer.

The local as well as average skin friction and Nusselt number in non-dimensional form are given by the following expressions:

$$\tau_X = -\left(\frac{\partial U}{\partial Y}\right)_{Y=0}, \tag{13}$$

$$\bar{\tau} = -\int_0^1 \left(\frac{\partial U}{\partial Y}\right)_{Y=0} \mathrm{d}X, \tag{14}$$

$$Nu_X = -X\left(\frac{\partial T}{\partial Y}\right)_{Y=0}, \tag{15}$$

$$\overline{Nu} = -\int_0^1 \left(\frac{\partial T}{\partial Y}\right)_{Y=0} \mathrm{d}X \tag{16}$$

The local and average skin friction are shown in Figs. 4, 5. It was observed that local skin friction increases with increasing the Prandtl number but decreases with an increasing Grashof number. The local wall shear stress decreases as M decreases. This is because of the fact that the velocity decreases near the plate as M increases. It is also observed that the local skin friction decreases with the decreasing value of radiation parameter N. The same trend is also noticed for average skin friction.

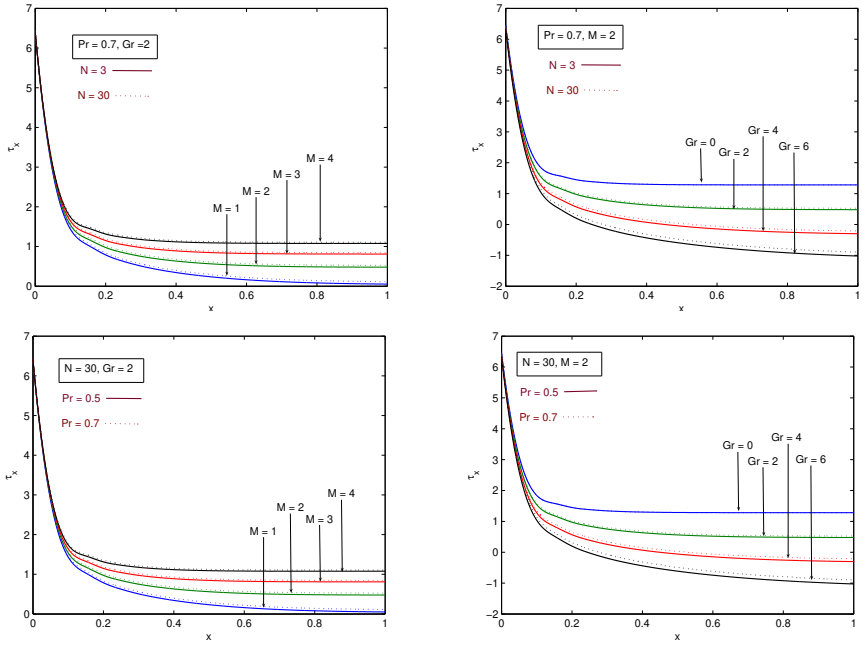

Fig. 4. Local skin friction.

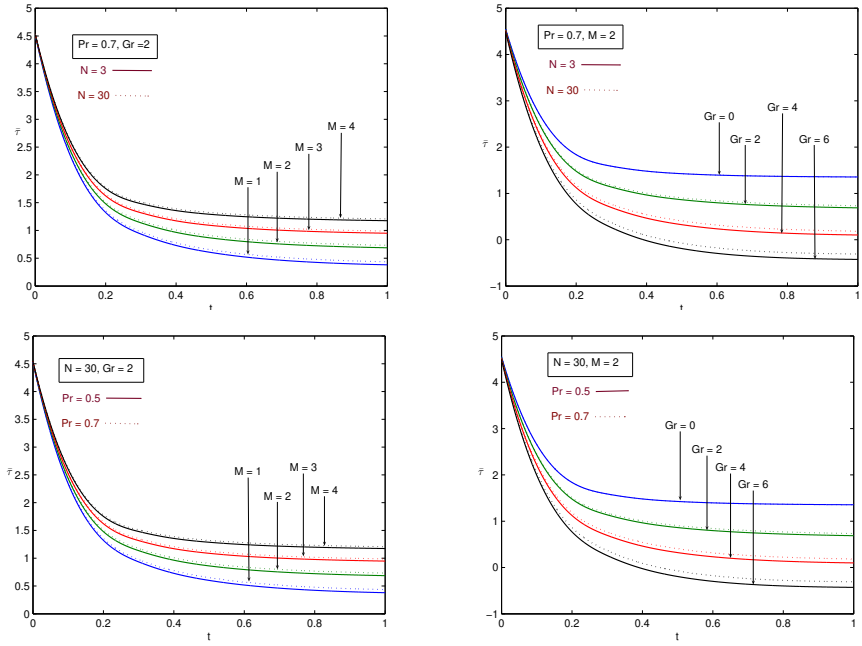

Fig. 5. Average skin friction.

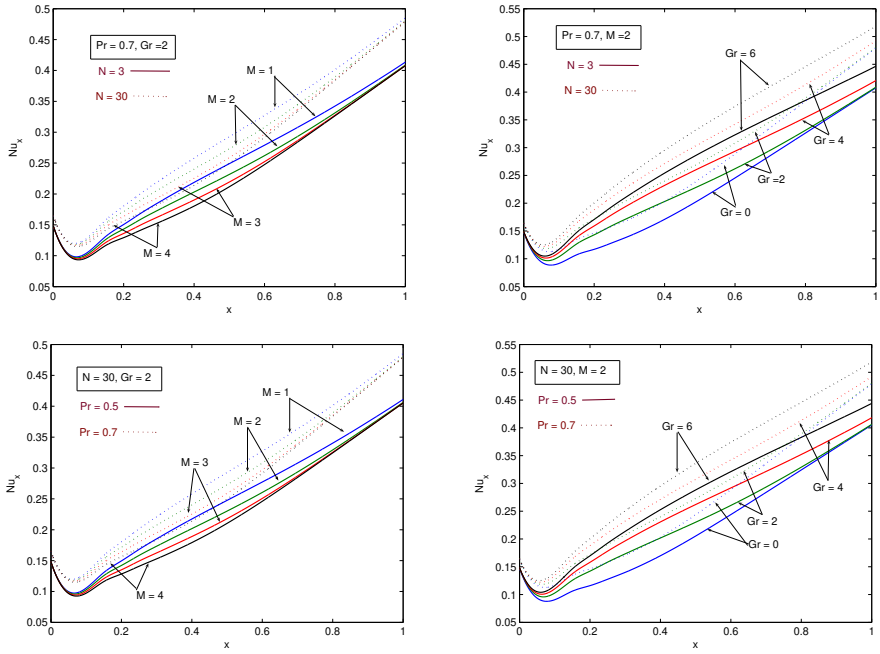

Fig. 6. Local Nusselt number.

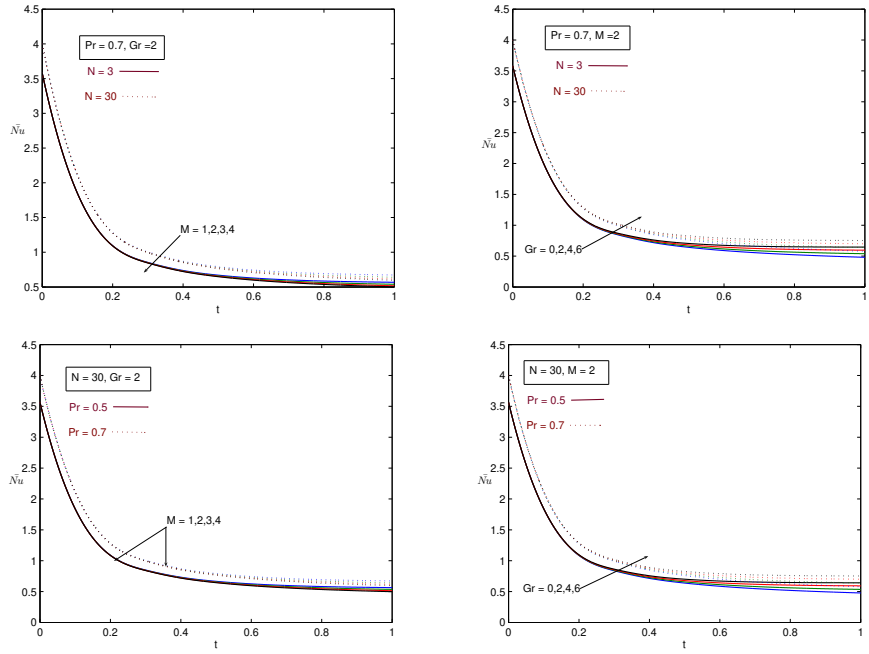

Fig. 7. Average Nusselt number.

The local and average Nusselt number were calculated numerically and are plotted in Figs. 6, 7. It was observed that local Nusselt number increases with an increasing Grashof number (or) decreasing magnetic field parameter. The local heat transfer was stronger on Pr than on the other parameters, since a lower Pr gives thicker temperature profiles. Larger values of Nusselt numberwere observed for higher values of Prandtl number.

In the initial time, higher values of average Nusselt numbers were observed. They decreased with time and become steady state after some time. Average Nusselt numbers were presented for various values of Pr, Gr, M and N. It was observed that for short times, the average Nusselt number was constant at each level of various parameters. This shows that initially there is only heat conduction. The average Nusselt number became reduced by the increasing value of the magnetic field parameter M. But it also gets reduced by the decreasing value of Grashof number (or) radiation parameter N. The average Nusselt number was found to decrease with the decreasing value of the Prandtl number of the fluid.

5 Conclusion

A Mathematical model has been presented for the unsteady convection heat transfer from a vertical plate with combined effects of MHD and thermal radiation. The governing boundary layer equations have been non-dimensionalised and solved using the finite element method. It has been shown that the velocity increases with a decreasing thermal radiation parameter (or) magnetic field parameter M. Dimensionless temperature is also seen to decreases owing to an increase in thermal radiation.

References

1. E. M. Sparrow, R. D. Cess, The effect of a magnetic field on free convection heat transfer, *Int. J. Heat Mass Tran.*, **3**(4), pp. 267–274, 1961.

2. R. D. Cess, The interaction of thermal radiation with free convection heat transfer, *Int. J. Heat Mass Tran.*, **9**(11), pp. 1269–1277, 1966.

3. V. M. Soundalgekar, S. K. Gupta, R. N. Arnake, Free convection effects on MHD Stokes problem for a vertical plate, *Nucl. Eng. Des.*, **51**, pp. 403–407, 1979.

4. V. M. Soundalgekar, M. R. Patil, M. D. Jahagirdar, MHD Stokes problem for a vertical plate with variable temperature, *Nucl. Eng. Des.*, **64**, pp. 39–42, 1981.

5. V. M. Soundalgekar, Mohammed Abdulla Ali, Free Convection effects on MHD flow past an impulsively started infinite vertical isothermal plate, *Reg. J. Energy Heat and Mass Transfer*, **8**(2), pp. 119–125, 1986.

6. M. Kumari, G. Nath, Development of two dimensional boundary layer with an applied magnetic field due to an impulsive motion, *Indian J. Pure Appl. Math.*, **30**, pp. 695–708, 1999.

7. K. Vajravalu, Hydromagnetic convection at a continous moving surface, *Acta Mech.*, **72**, pp. 223–232, 1988.

8. V. M.Soundalgekar, H. S. Takhar, Radiation effects on free convection flow past a semi-infinite vertical plate, *Modelling Measurement and Control*, **B51**, pp. 31–40, 1993.

9. M. A.Hossain, H. S. Takhar, Radiation effects on mixed convection along a vertical plate with uniform surface temperature, *Heat Mass Transfer*, **31**, pp. 243–248, 1996.

10. A. Raptis, C. Perdikis, Radiation and free convection flow past a moving plate, *Int. J. of Applied Mechanics and Engineering*, **4**(4), pp. 817–821, 1999.

11. R. Muthucumaraswamy, P. Ganesan, Radiation effects on flow past an impulsively started infinite vertical plate with variable temperature, *Int. J. of Applied Mechanics and Engineering*, **8(1)**, pp. 125–129, 2003.

12. A. Raptis, C. V. Massalas, Magnetohydrodynamic flow past a plate by the presence of radiation, *Heat Mass Transfer*, **34**, pp. 107–109, 1998.

13. H. S. Takhar, O. A. Beg, A. J. Chamkha, D.Filip, I.Pop, Mixed radiation-convection boundary layer flow of an optically dense fluid along a vertical flat plate in a non-Darcy porous medium, *Int. J. of Applied Mechanics and Engineering*, **8**(3), pp. 483–496, 2003.

14. O. Anwar Beg, J. Zueco, H. S. Takhar, T. A. Beg., Network Numerical simulation of impulsively-started transient radiation-convection heat and mass transfer in a saturated Darcy-Forchheimer porous medium, *Nonlinear Anal. Model. Control*, **13**(3), pp. 281–303, 2008.

15. M. Q. Brewester, *Thermal Radiative Transfer and Properties*, New York, John Wiley and Sons, Inc, 1992.

16. K. J. Bathe, *Finite Element Procedures*, Prentice-Hall, New Jersey, 1996.